1970

Electron optical study of a secondary electron multiplier

Chang Min Shen
Portland State University

AN ABSTRACT OF THE THESIS OF Chang Min Shen for the Master of Science in Physics presented July 24, 1970.

Title: Electron Optical Study of a Secondary Electron Multiplier.

APPROVED BY MEMBERS OF THE THESIS COMMITTEE:

[redacted]

Friedrich A. Lenz, Chairman

[redacted]

Gertrude F. Rempfer

[redacted]

Michael A. Philippas

Electron optical theory was applied to the design of the geometrical structure of an electron multiplier for an image intensifier. A special structure satisfying production requirements was studied. Electron optical calculations consisted of determining the potential distribution and tracing the electron trajectories. Liebmann's procedure was used to solve Laplace's equation with constant potentials on the multiplier electrodes as boundary conditions. The trajectories were determined by solving the equation of motion in an

electrostatic field using a Runge-Kutta procedure. The initial conditions for the trajectories were the initial energies, initial positions, and the initial directions of the secondary electrons. The plotted trajectories indicated the feasibility of an electron multiplier of the type studied.

ELECTRON OPTICAL STUDY OF A SECONDARY ELECTRON MULTIPLIER

by

CHANG MIN SHEN

A thesis submitted in partial fulfillment of the requirements for the degree of

MASTER OF SCIENCE

in

PHYSICS

Portland State University

1970

TO THE OFFICE OF GRADUATE STUDIES:

The members of the committee approve the thesis of Chang Min Shen presented July 24, 1970.

[redacted]

Friedrich A. Lenz, Chairman

[redacted]

Gertrude F. Rempfer

[redacted]

Michael A. Philippas

APPROVED:

[redacted]

Mark Gurevitch, Head, Department of Physics

[redacted]

David T. Clark, Dean of Graduate Studies

TABLE OF CONTENTS

LIST OF FIGURES

INTRODUCTION

An electron multiplier is a device by which an input electron current can be multiplied greatly at its output. The ratio of the electron current at the output to that at the input is called the gain of the multiplier. An electron multiplier usually has a number of electrodes, known as dynodes. The surfaces of the dynodes are coated with a material having a high secondary emission coefficient. When primary electrons hit the first dynode with sufficient energy (e.g. 100 electron-volts or more), secondary electrons, whose number may exceed the number of the primaries, are emitted. These electrons, in turn, are accelerated to the second dynode by the voltage applied between the first and second dynodes, where they again release secondaries. If this is continued, the number of secondary electrons at the output of the last dynode can be much greater than the input to the first dynode.

An application of the electron multiplier in a cathode ray tube is to improve its performance at high sweeping speed. With increasing sweeping speed in a CRT, the trace on the screen becomes weaker, because

of the decrease in the electron density on the screen. A multi-channel electron multiplier in front of the screen can increase the electron current density greatly, and hence the brightness of the trace. Such a multiplier consists of a great number of small single channel multipliers as mentioned above. All of the first electrodes of the small multipliers form a honeycomb-like mesh structure in a planar first stage of the multiplier. Similarly, the second stage consists of all of the second dynodes, and so on. Usually there are four to ten stages in such a multi-channel beam current multiplier.

In this paper, a multiplier with a conical hole type structure is described. Figure 1(a) shows the structure of a single channel multiplier. The larger side of the hole faces the incoming electrons. The inner walls of the holes are coated with a material having a high coefficient of secondary emission. Figure 1(b) shows a part of the honeycomb structure and Figure 1(c) the cross section SS of the structure shown in 1(b). The spacing is defined as the distance from the bottom of a stage to the top of the next stage.

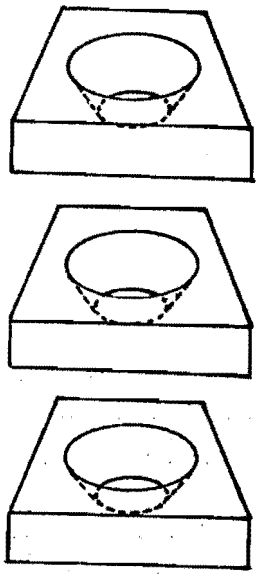

(a) Structure of single channel multiplier.

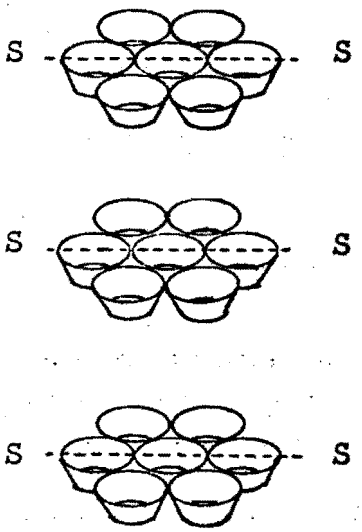

(b) Honeycomb structure.

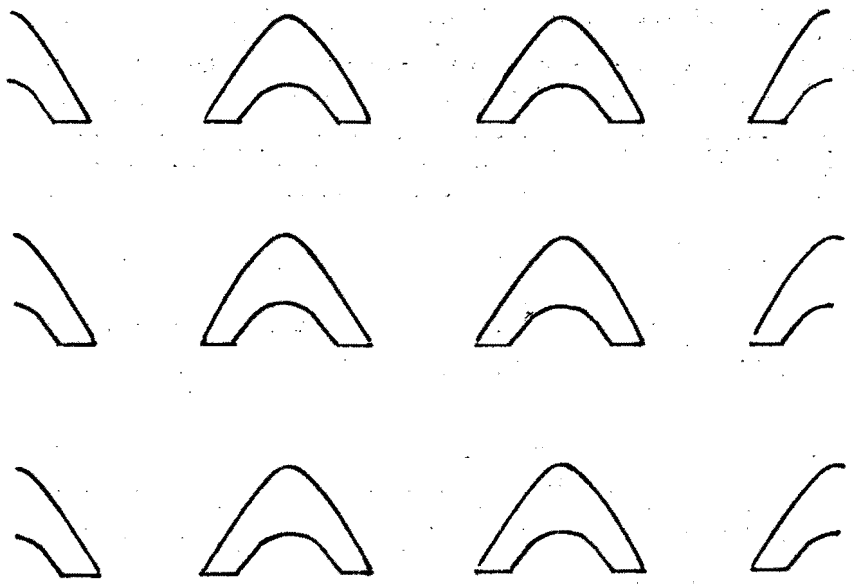

(c) Cross section of the honeycomb structure.

Figure 1. Structure of the multiplier

The main purposes of this paper are: (1) to seek a theoretical basis for the multiplier structure, and (2) to obtain maximum gain by optimizing the spacing between the stages. In order to solve these problems, the potential distribution in the field and some electron trajectories were calculated. It is essential for the function of the multiplier that most of the secondary electrons emitted from one stage should neither miss the next stage nor hit the original stage, but go from each stage to the next one. To obtain maximum gain, the spacing must be so chosen that most of the secondary electrons from one stage not only go to the next stage but to its active region. The active region is the region on the inner wall surface from which secondary electrons have a good chance to reach the next stage.

The trajectory of an electron depends on the potential distribution and on the initial conditions, i.e. the point of origin and the initial energy and direction of the electron. These factors which influence the trajectories are discussed separately:

1. THE POTENTIAL DISTRIBUTION

The potential distribution depends on the shapes and the potentials of the electrodes.

In the present study, the only shape parameter varied was the spacing between stages while the shapes of the single stages, shown in Figure 2, were not changed. The electrode dimensions and the spacing are given in terms of an arbitrary length unit h, since, for the calculation of the potential distribution and the trajectories, it is not necessary to know the absolute lengths. The potential distribution has been calculated for three different values of the spacing relative to the electrode dimensions.

2. THE POINT OF ORIGIN

The probability of a secondary electron reaching the next stage depends strongly on the position from which it is emitted. Close to the lower edge of the inner wall surface, the electric field pulls the secondaries away from the surface and down through the hole. Farther away from the edge, the field at the surface has the opposite direction, pushing most of the slow secondaries back to the surface, so that they cannot contribute to the gain. Therefore, the active region is a band

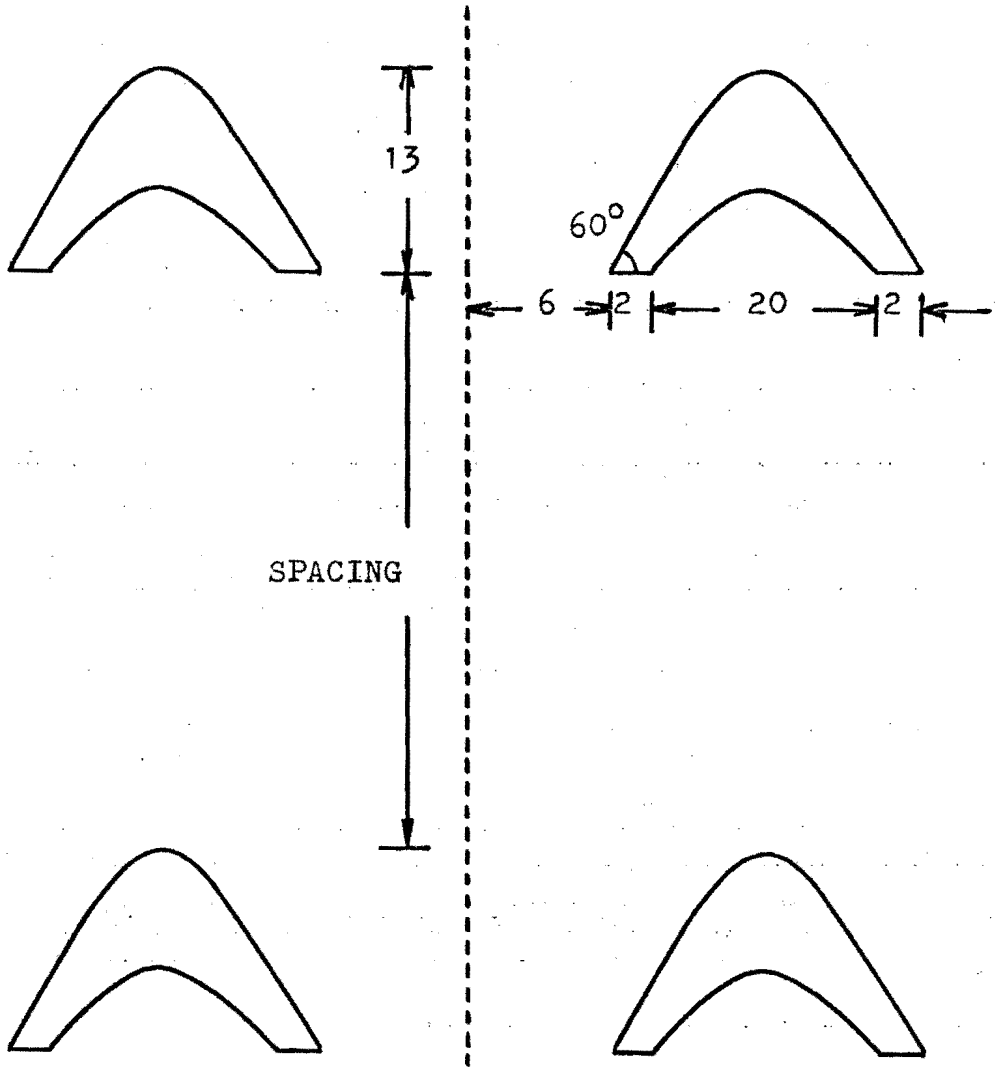

Figure 2. Shape and dimensions of the multiplier. (Unit of length is arbitrary)

of limited width close to the lower edge, while the local gain in the remaining surface region is negligible. Figure 3 shows qualitatively the dependence of local gain on the radial coordinate in the hole. The equipotential surface which meets the upper stage at right angles, separates the two regions on the inner wall which have different signs of the electric field strength at the surface.

3. THE INITIAL ENERGY OF THE SECONDARY ELECTRONS

Electrons with higher initial energies have less curved trajectories than electrons with lower initial energies. In the active region, electrons with all initial energies can leave the surface. In the upper, inactive region, trajectories must have sufficient initial evergy to surpass the energy barrier of the retarding field.

4. THE INITIAL DIRECTION

The initial direction of each secondary electron can be described by two angles α and β . α is the angle between the initial direction and the direction of the axis (Figure

4(a)). β is the angle between the projection of the initial direction on a plane perpendicular to the axis and the meridional plane, I.E. the plane through the point of emission and the axis (Figure 4(b)).

Meridional rays ($\beta = 0^\circ$ or 180°) are plotted in the meridional plane. Since a three-dimensional ("skew") trajectory in general does not lie in a plane, its geometrical properties cannot be completely represented in a two-dimensional plot. One way of representing it is to show two or more projections, e.g. on the meridional plane through the axis and the point of origin and on the plane through the axis but perpendicular to the first one, or on a plane perpendicular to the axis. For the present study, it was considered sufficient to plot the radial coordinate r as a function of the axial coordinate z. It should, however, be borne in mind that a strong curvature in a r(z) plot does not necessarily mean that the trajectory itself is strongly curved.

The calculation of the field and of the trajectories is much simplified by the periodicity of the

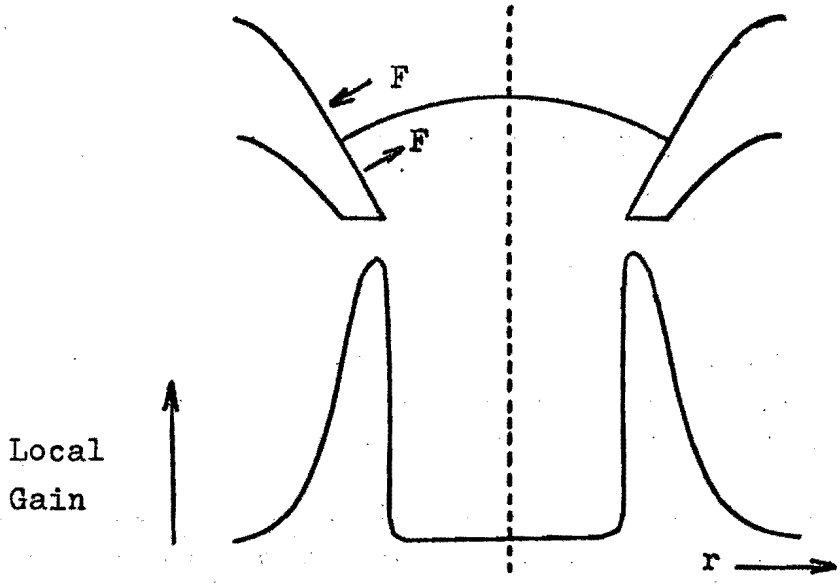

Figure 3. Local gain of the multiplier stage.

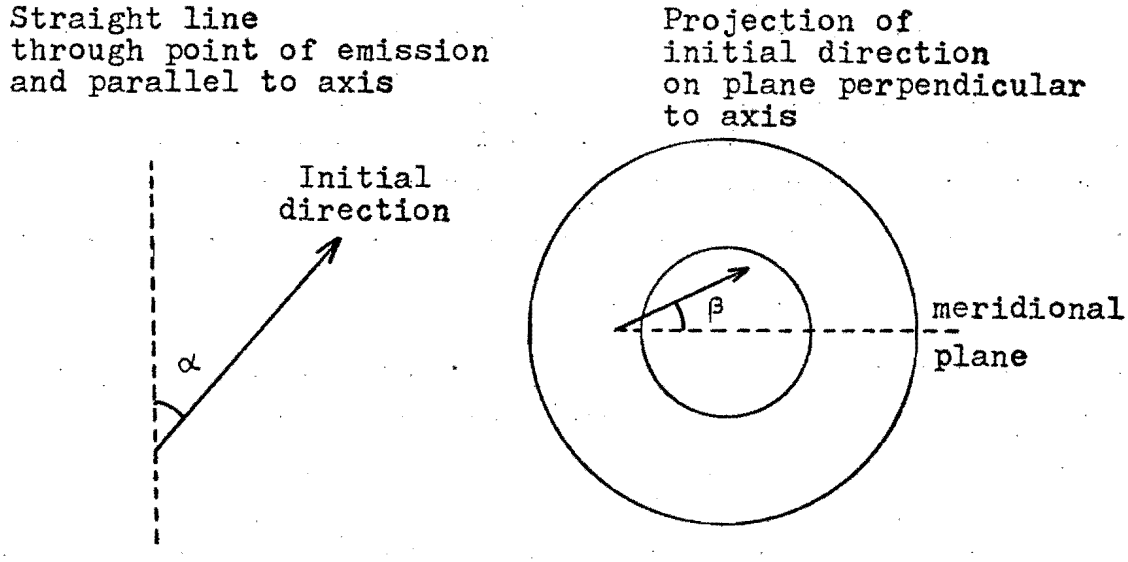

(a) Plane parallel to the axis and containing initial direction.

(b) Plane perpendicular to axis.

Figure 4. Parameters and describing the initial direction of the secondary electrons.

structure. The potential at a point in the n-th stage is equal to the potential of the equivalent point in the m-th stage plus (n-m) times the potential difference between two subsequent stages. A trajectory of an electron from a point on the surface of the n-th stage has the same shape as the trajectory of an electron emitted from the m-th stage with equivalent initial conditions. It is only shifted in the z direction by (n-m) times the periodicity length of the stages in this direction. Corresponding periodicity relations are valid in the sidewise direction so that it is sufficient to study the potential distribution and the trajectories in one periodicity element. Of course, the first and the last stages are exceptions, as far as the periodicity relations are concerned.

THE SECONDARY EMISSION PROPERTIES OF THE MULTIPLIER

The secondary yield (δ) is defined as the ratio of the average number of electrons that leave a surface to the number of electrons that bombard it. δ depends on (1) the material of the surface, (2) the energy of the bombarding (primary) electrons, and (3) the angle of incidence of the primary electrons.

The secondary electrons have a distribution of initial energy. Figure (5) shows qualitatively this distribution $f(\mathcal{E})$ where $f(\mathcal{E})d\mathcal{E}$ is the fraction of electrons having energies between $\mathcal{E}$ and $\mathcal{E}+d\mathcal{E}$. The electrons in the sharp peak at the right side of the energy spectrum are the reflected primaries which have not lost much energy. $\mathcal{E}_o$ is the most probable energy of the primary electrons. The electrons corresponding to peak at the left side are the so-called true secondary electrons. They are knocked out by the high velocity primaries. The distribution has a maximum lying in the range of 2 to 5 electron-volts. The position of the maximum on the energy axis is independent of the energy of the primaries, provided their energy is large compared with the energy spread of the true secondaries.

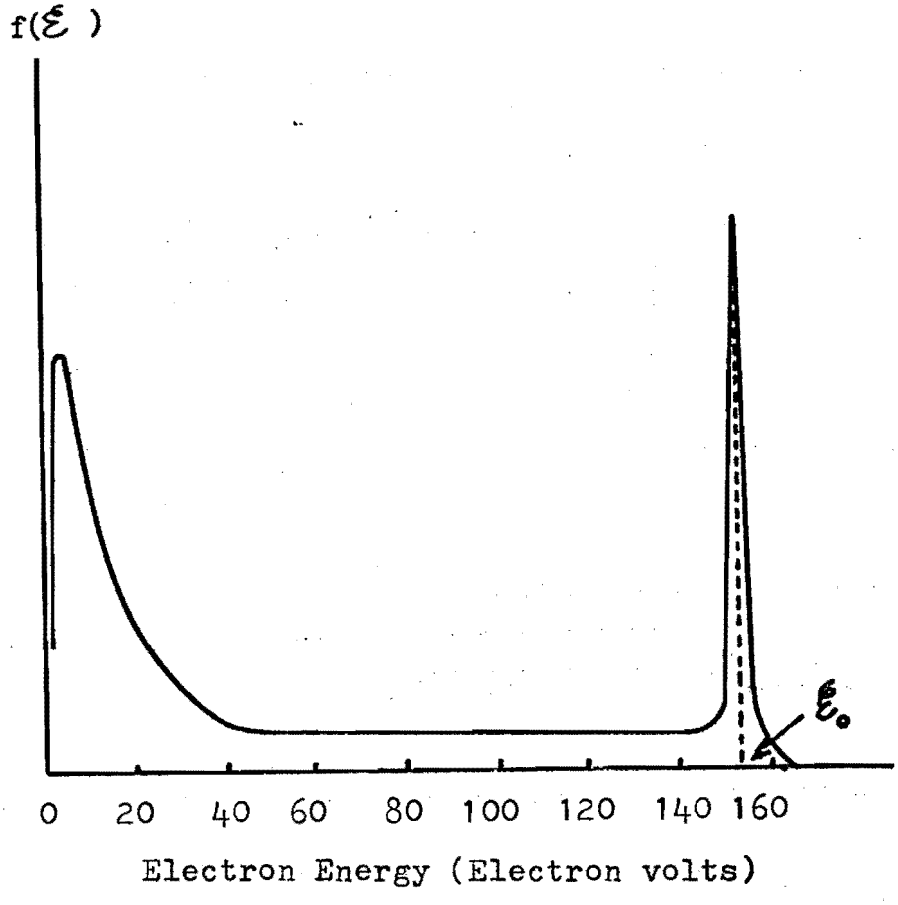

Figure 5. Typical energy distribution of secondary electrons. (Du Mont Multiplier and Specification, Second Edition, 1960.)

The reflected primaries do not contribute much to the function of the electron multiplier because they, as a result of their high energy, travel along almost straight lines between the stages and are hardly bent by the electric field between the stages. Therefore, our attention will be directed to the true secondary electrons. Furthermore, we are most interested in the electrons emitted normal to the surface, because the number of electrons emitted in a direction making an angle θ with the normal is proportional to $\cos\theta$.

THE DETERMINATION OF THE POTENTIAL DISTRIBUTION

Since neither the potential distribution nor the trajectories can be written in the form of simple mathematical functions, numerical method must be employed.

Liebmann's numerical method (Southwell 1956) of calculating the potential distribution in an electrostatic field consists of replacing the derivatives in Laplace's equation by finite differences of the potentials at a great number of equidistant mesh points in a quadratic mesh system stretched over the field. Relations between the potential at each mesh point and the potential at its neighboring mesh points are used to perform successive iterations converging towards a final solution which approximates the potential distribution. The choice of mesh size depends on the fineness of detail of the potential distribution needed. The smaller the size, the more accurate the distribution. However, smaller mesh size means a greater number of mesh points, and hence more potential values to be determined. This also means that more time is needed for the calculation. The number of points is inversely proportional to the square of the mesh size, and the number of iterations required increases even faster. To compensate for this drawback, a practical method is to have a smaller mesh size in the regions of strong field variation and a

larger one in the regions with a more homogeneous field. One of the three potential distributions calculated in this paper (the 33-unit spacing, see Appendix D) was done in this way with a desk calculator.

However, if the calculation is to be done by a computer, the mixed mesh size arrangement needs more programming time than a smaller uniform mesh system. When this is weighed against the actual computer time, the smaller uniform mesh system is less costly. The other two calculations of the potential distribution were done by this method (Appendices B and C). The arbitrary length unit mentioned on page 4 was chosen equal to the mesh size in this case.

The numerical method used is based on Laplace's equation in cylindrical coordinates (Becker 1964), which in this case of rotational symmetry is:

$$\frac{\partial^2\phi}{\partial r^2}+\frac{1}{r}\frac{\partial\phi}{\partial r}+\frac{\partial^2\phi}{\partial z^2}=0 \qquad (1)$$

For the different cases listed below, Liebmann's procedure yields the following finite difference formulas with mesh size h:

1. In general, except for the special categories following,

$$\phi(r,z)=\frac{1}{4}\left[\phi(r+h,z)+\phi(r-h,z)+\phi(r,z+h)+\phi(r,z-h)\right]$$
$$+\frac{h}{8r}\left[\phi(r+h,z)-\phi(r-h,z)\right] \qquad (2)$$

2. On the axis

$$\phi(0,z)=\frac{1}{6}\left[4\phi(h,z)+\phi(0,z+h)+\phi(0,z-h)\right] \qquad (3)$$

3. On the outer boundary with respect to r if the equipotentials are perpendicular to the boundary $\left(\frac{\partial\phi}{\partial r}=0\right)$

$$\phi(r,z)=\frac{1}{4}\left[2\phi(r-h,z)+\phi(r,z+h)+\phi(r,z-h)\right] \qquad (4)$$

4. At the boundaries in the z-direction, formula (2) cannot be applied immediately because no potential values are available at mesh points beyond the boundaries. If there is a total of n meshes along the z-axis in one of the regions as shown in Figure 1(c), then from Figure 6, the potential at z=-h differs from that at z=(n-1)h by the constant accelerating voltage ϕ_0 between the successive stages. Thus we have

$$\phi(r,-h)=\phi(r,(n-1)h)-\phi_0 \qquad (5)$$

Correspondingly, we have

$$\phi(r,-2h)=\phi(r,(n-2)h)-\phi_0 \qquad (6)$$

$$\phi(r,(n+1)h)=\phi(r,h)+\phi_0 \qquad (7)$$

Equations (5) to (7) are used to supply the potentials at the mesh points beyond the boundary.*

---

*This method of replacing boundary conditions by a condition of periodicity has not to our knowledge been described elsewhere.

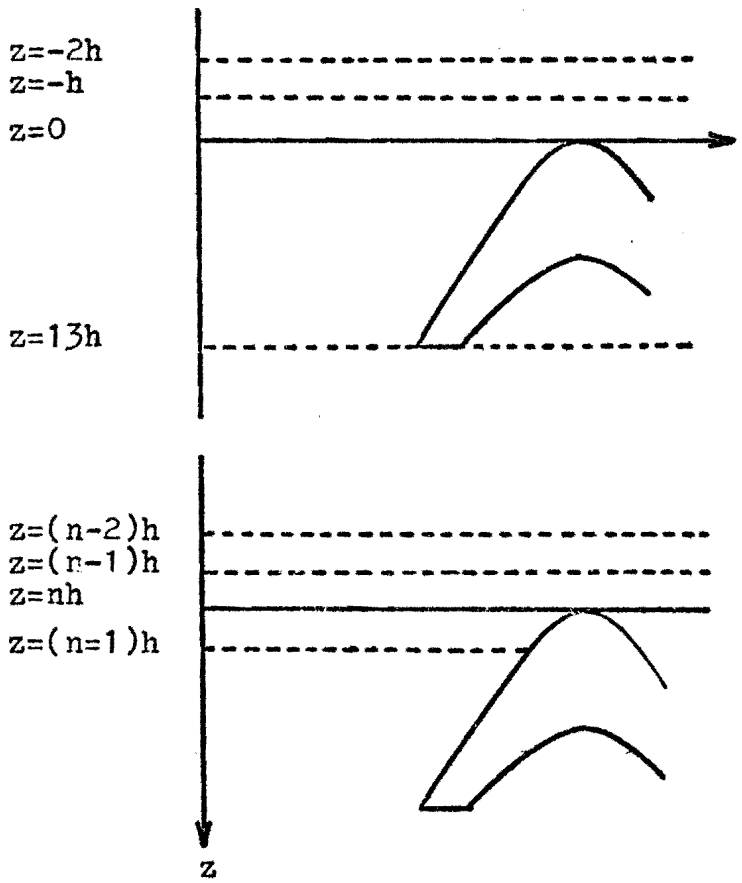

Figure 6. Periodicity of potential along z-axis.

5. When the electrode does not intersect the mesh lines in integer mesh points, formula (2) cannot be applied at points close to the electrode. The potentials at such points are determined by interpolation. The potential at a point a distance ah ($0<a<1$) from the electrode along the r-axis is determined using a three-point Lagrange interpolation formula (Abramowitz, et al., 1964) (Figure 7).

$$\phi=\frac{2}{(1+a)(2+a)}\phi_c+\frac{2a}{1+a}\phi_1-\frac{a}{2+a}\phi_2 \qquad (8)$$

As a special case, if $\phi_c=0$, (8) becomes

$$\phi=\frac{2a}{1+a}\phi_1-\frac{a}{2+a}\phi_2 \qquad (9)$$

This is the interpolation formula used in this paper, and it can be applied to either the r or the z coordinate. In case the potential at a point can be found by applying interpolation to either the r or the z coordinate, the coordinate corresponding to the smaller "a" value is chosen.

6. The potentials at points close to a sharp edge of the electrode, e.g. the bottom rim in our case, should not be calculated by one of the foregoing formulas. This is because, at such a sharp edge,

the field strength becomes infinite while the potential remains finite. Assume that γ is the angle (in radians) of the sharp edge and that this edge coincides with an integer mesh point (r,z), as shown in Figure 8. An analysis from a solution of Laplace's equation gives (Lenz 1968)

$$\phi(r-h,z)=\left(\frac{1}{2}\right)^{\pi/(2\pi-\gamma)}\phi(r-2h,z)-\left[1-\left(\frac{1}{2}\right)^{\pi/(2\pi-\gamma)}\right]\phi(r,z)$$

In our case, $\gamma=\frac{\pi}{3}$, we have

$$\frac{\pi}{2\pi-\gamma}=\frac{3}{5}=0.6$$

and

$$\phi(r-h,z)=\left(\frac{1}{2}\right)^{0.6}\phi(r-2h,z)+\left[1-\left(\frac{1}{2}\right)^{0.6}\right]\phi(r,z)$$

$$=0.6598\,\phi(r-2h,z)+0.3402\,\phi(r,z)$$

If $\phi(r,z)=0$, we have

$$\phi(r-h,z)=0.6598\,\phi(r-2h,z) \qquad (10)$$

Similarly, for the point which is one mesh space from the sharp edge along the z-axis, we have

$$\phi(r,z+h)=0.6598\,\phi(r,z+2h) \qquad (11)$$

The formulas (2) through (11) are used for the calculation of the potentials at the integer mesh points. Each of them applies to a different type of location.

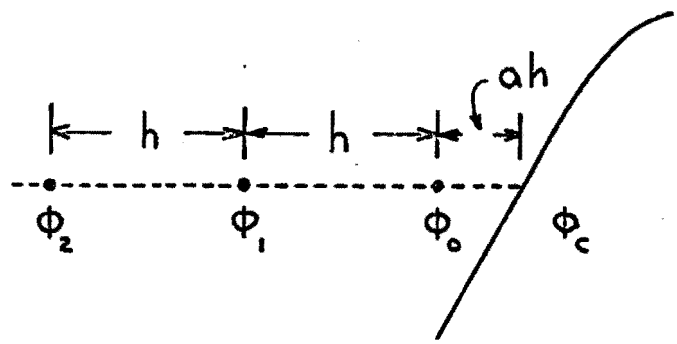

Figure 7. Interpolation of the potentials.

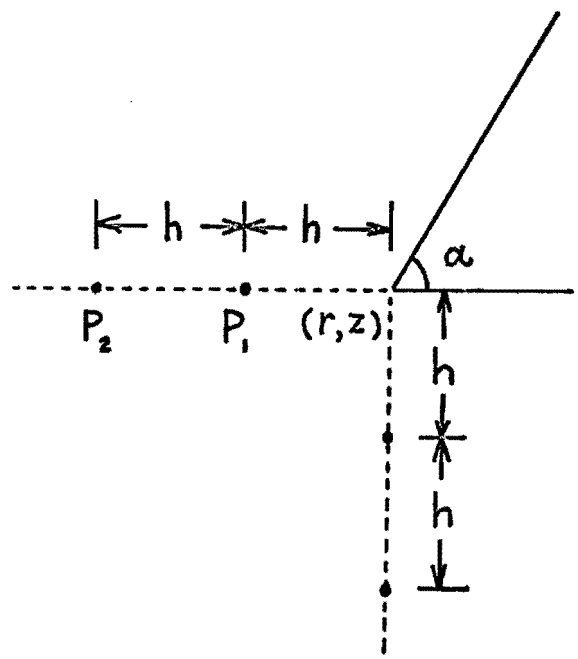

Figure 8. Potentials at the neighborhood of a sharp edge of the electrode.

A crude guess of the potential distribution is used to obtain the next approximation, and so on. This iterative procedure is continued until the greatest change of any potential value per iteration becomes small compared with the desired accuracy.

The order in which the new potentials in the different mesh points are calculated has no effect on the result, but each mesh point should be treated in each iteration. In this computation, the mesh points were scanned radially outward starting from the z-axis. An entire sweep over the field from z=n to z=0 constitute one iteration. Almost any initial approximation satisfying the boundary condition can be used because the potentials converge during the calculation. However, a good guess reduces the calculation time. Starting from a rough approximation, usually between two and three hundred iterations were needed to obtain an accuracy of the order of 0.01%.

In this paper, the initial potentials at the integer mesh points in the space from z=0 to z=13 were assumed to be zero, the potential of the electrode. In the space from z=13 to z=n, the potential was set equal to

$$\frac{z-13}{n-13}\phi_o ,$$

i.e. a homogenious field was assumed.

Because of the linearity of Laplace's equation, the potentials at the upper and at the lower electrodes of a stage may be chosen arbitrarily. For convenience, the calculation was performed with a potential value of zero for the upper and 10,000 units for the lower electrode. If the corresponding solution is $\phi(r,z)$, then a solution, where the upper stage is at V and the lower at $V+\phi_o$, is

$$V+\phi_o \frac{\phi(r,z)}{10,000}$$

The potential distribution $\phi(r,z)$ was calculated for the cases n=23, n=32, and n=46 corresponding to spacings 10, 19, and 33, respectively. Appendix A contains the computer (IBM 1130) program used for the calculation of the potential distribution. Appendices B, C, and D are the final converged distributions for 10-, 19-, and 33-unit spacings, and Figures 9 and 10 show the equipotential plots for the cases of 10-unit (n=23) and 19-unit (n=32) spacings.

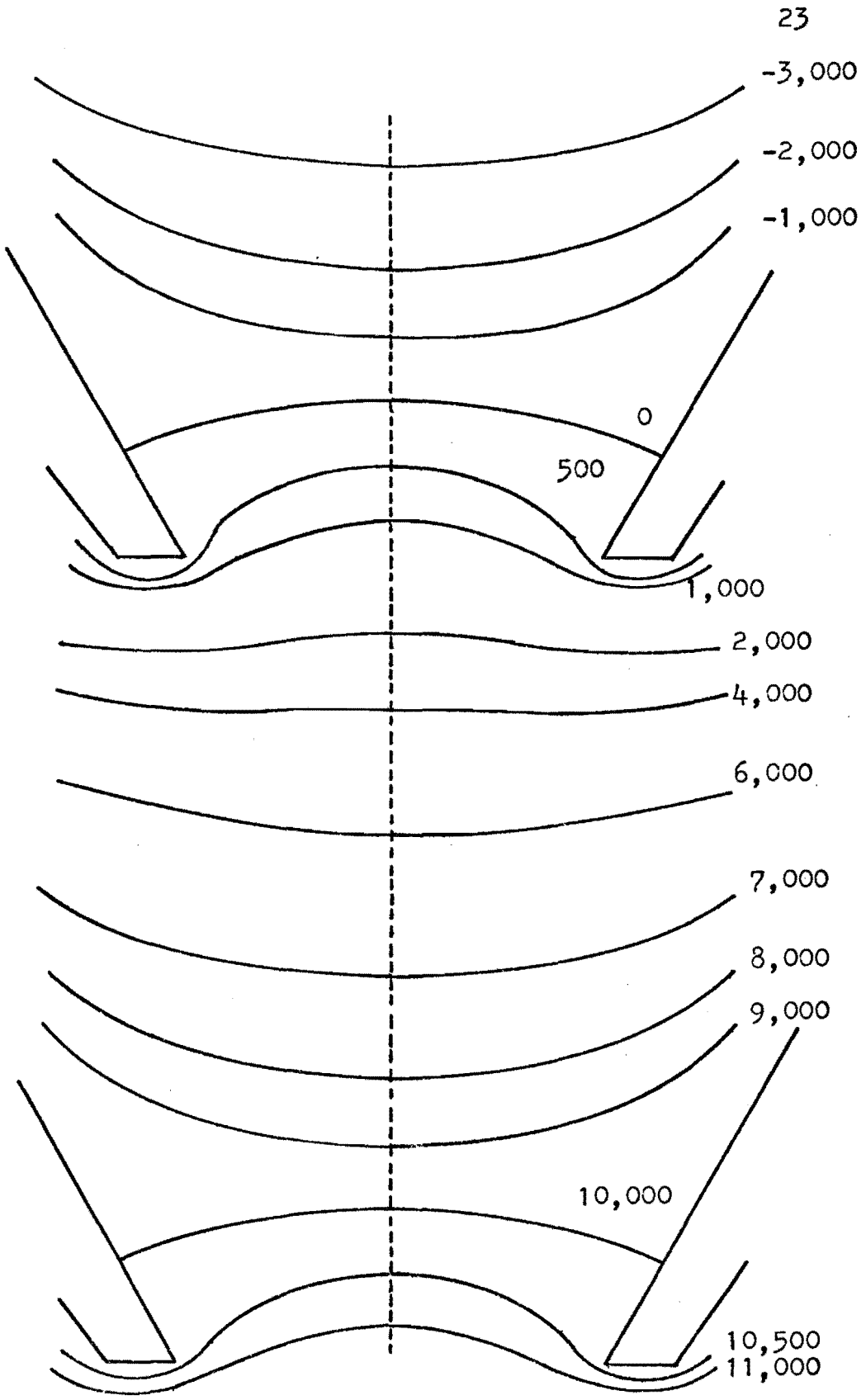

Figure 9. Equipotentials for 10-unit spacing (n=23)

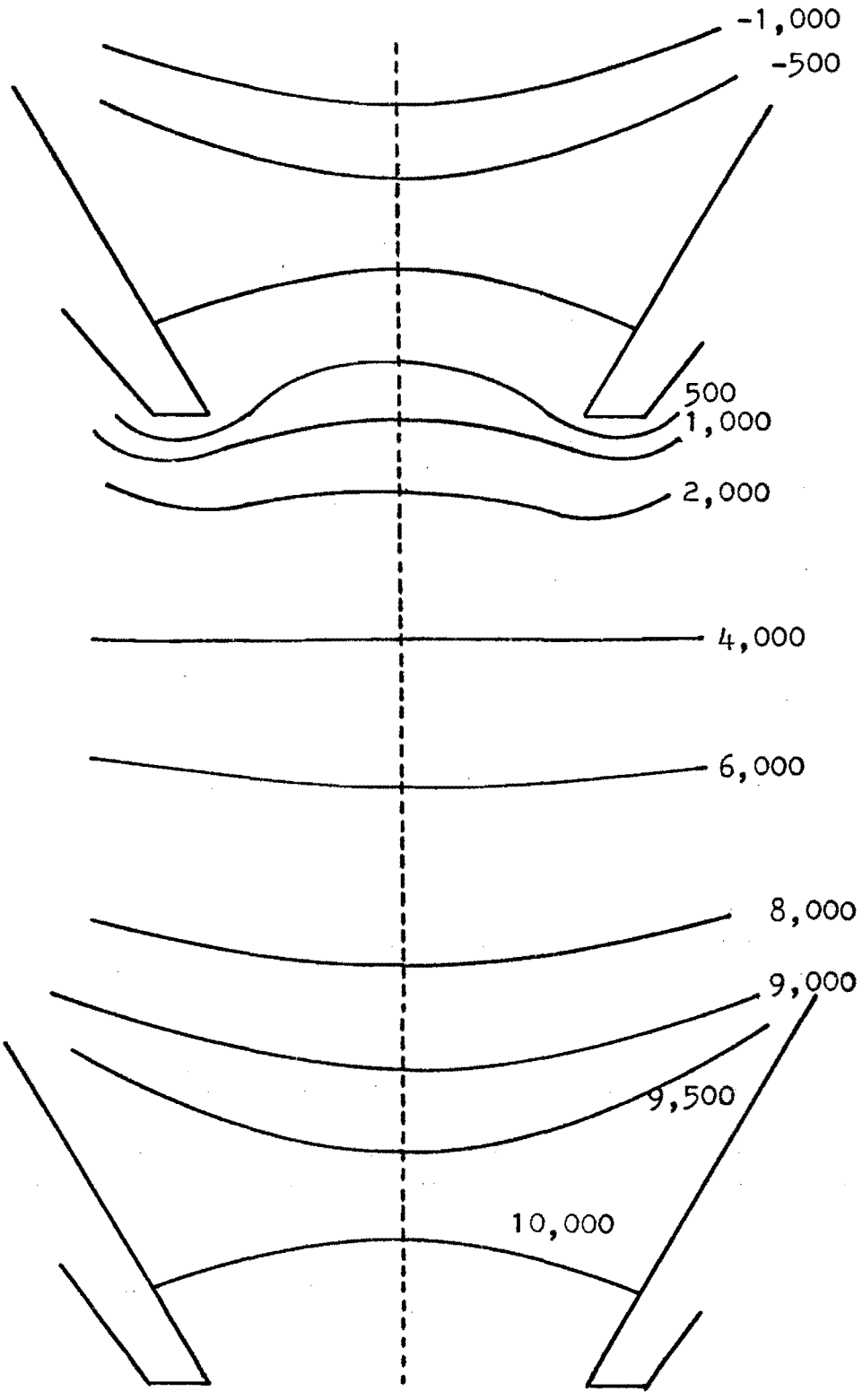

Figure 10. Equipotentials for 19-unit spacing (n=32).

THE PLOT OF THE TRAJECTORIES

The equation of motion of non-relativistic electrons in an electrostatic field is

$$m\frac{d^2\vec{r}}{dt^2} = e\nabla\phi(\vec{r}) \qquad (12)$$

where m and e are the mass and charge of the electron, respectively. As our interest is in the geometrical properties of the trajectories and not the dependence of the trajectory coordinates on time t, we may eliminate the operator $\frac{d}{dt}$ by using

$$v\frac{d}{ds} = \frac{d}{dt}$$

where v is the velocity of the electron and s the path length. Substituting into (12), we have

$$mv\frac{d}{ds}\left(v\frac{d\vec{r}}{ds}\right) = e\nabla\phi(\vec{r}) \qquad (13)$$

In this non-relativistic problem, we have

$$v = \sqrt{\frac{2e}{m}(\phi + E)}$$

where eE is the total energy of the electron. Substituting into (13), we get

$$\sqrt{2(\phi+E)}\,\frac{d}{ds}\left(\sqrt{2(\phi+E)}\,\frac{d\vec{r}}{ds}\right) = \nabla\phi(\vec{r}) \qquad (14)$$

If this vector equation is written in Cartesian components, we have

$$2\sqrt{\phi+E}\,\frac{d}{ds}\left(\sqrt{\phi+E}\,\frac{dx}{ds}\right)=\frac{\partial\phi}{\partial x}$$

$$2\sqrt{\phi+E}\,\frac{d}{ds}\left(\sqrt{\phi+E}\,\frac{dy}{ds}\right)=\frac{\partial\phi}{\partial y} \qquad (15)$$

$$2\sqrt{\phi+E}\,\frac{d}{ds}\left(\sqrt{\phi+E}\,\frac{dz}{ds}\right)=\frac{\partial\phi}{\partial z}$$

In our cylindrically symmetrical problem, ϕ does not depend on the azimuth angle Ψ . Thus

$$\frac{\partial\phi}{\partial x}=\frac{\partial\phi}{\partial r}\frac{\partial r}{\partial x}=\frac{x}{r}\frac{\partial\phi}{\partial r}=\frac{x}{\sqrt{x^2+y^2}}\frac{\partial\phi}{\partial r}$$

Similarly,

$$\frac{\partial\phi}{\partial y}=\frac{\partial\phi}{\partial r}\frac{\partial r}{\partial y}=\frac{y}{r}\frac{\partial\phi}{\partial r}=\frac{y}{\sqrt{x^2+y^2}}\frac{\partial\phi}{\partial r}$$

Substituting into (15), we get

$$2\sqrt{\phi+E}\,\frac{d}{ds}\left(\sqrt{\phi+E}\,\frac{dx}{ds}\right)=\frac{x}{\sqrt{x^2+y^2}}\frac{\partial\phi}{\partial r}$$

$$2\sqrt{\phi+E}\,\frac{d}{ds}\left(\sqrt{\phi+E}\,\frac{dy}{ds}\right)=\frac{y}{\sqrt{x^2+y^2}}\frac{\partial\phi}{\partial r}$$

$$2\sqrt{\phi+E}\,\frac{d}{ds}\left(\sqrt{\phi+E}\,\frac{dz}{ds}\right)=\frac{\partial\phi}{\partial z}$$

This system of three ordinary non-linear second-order differential equations can be transformed into a system of six ordinary non-linear first order differential equations:

$$\frac{dx}{ds}=\frac{1}{\sqrt{\Phi+E}}p\;;\quad \frac{dp}{ds}=\frac{1}{2\sqrt{\Phi+E}}\frac{x}{\sqrt{x^2+y^2}}\frac{\partial\Phi}{\partial r}$$

$$\frac{dy}{ds}=\frac{1}{\sqrt{\Phi+E}}q\;;\quad \frac{dq}{ds}=\frac{1}{2\sqrt{\Phi+E}}\frac{y}{\sqrt{x^2+y^2}}\frac{\partial\Phi}{\partial r} \qquad (16)$$

$$\frac{dz}{ds}=\frac{1}{\sqrt{\Phi+E}}u\;;\quad \frac{du}{ds}=\frac{1}{2\sqrt{\Phi+E}}\frac{\partial\Phi}{\partial z}$$

From here, the trajectories were computed by a Fortran computer program using the Runge-Kutta procedure (Lenz 1970). In this program, the initial Cartesian coordinates x, y, and z, the total energy, and the two parameters α and β (Figure 4) defining the initial direction are input. The step width along the trajectory is also input. It can be changed during a trajectory run. The potential distributions were supplied by the computer program described in Appendix A.

The printout of the result of the calculation of the trajectories from the computer contains a set of four coordinates, x, y, z, and r. The meridional trajectories for which y=0 are plotted in the xz-plane. The skew trajectories are plotted in cylindrical coordinates r and z. Figures 11 to 19 show some trajectories for spacings of 10, 19, and 33 mesh units.

Figure 11 shows the meridional trajectories in

a model with a spacing between stages of 19 mesh units. The secondary electrons were assumed to have initial energies of 3% of the accelerating voltage and initial directions normal to the surface. This plot shows the effect of the emitting position on the trajectories. The closer the emitting point to the edge, the farther from the edge of the next stage is the landing point of the trajectory. Trajectory 4 misses the next stage and trajectory 5 returns back to the original stage.

Figure 12 and 13 show trajectories with different initial energies, initially normal to the surface. In the 33-unit spacing model, Figure 13, the trajectories with 4% and 5% initial energies went to the opposite wall of the original stage. Only electrons with energies less than somewhere between 3% and 4% could go to the next stage. However, in Figure 12, a plot of the 10-unit spacing model, electrons with initial energies up to much more than 4% go to the next stage. It appears that only electrons with very high initial energies would be stopped by the original stage, but their number can be assumed to be very small. Trajectories for the 19-unit spacing model are shown in Figure 14.

Trajectories 1 and 3 which are initially normal to the surface can be compared with the trajectories of the 10-unit spacing model. They land in a less sensitive region farther from the edge of the next stage. Thus, as far as the secondary electron gain is concerned, the 10-unit spacing model is the best among the three.

The trajectories 2, 3, and 4 in Figure 14 are meridionals in the 19-unit spacing model with the same initial energy of 3%, but with different values of the angle α. The trajectories with different α values cross each other, forming an envelope. An envelope is also formed by trajectories 2, 3, and 4 in Figure 15, which are emitted from a different point (r_o=8). Figure 16 shows some trajectories for the 10-unit spacing model. The trajectories 1 and 2 are meridionals emitted from point r_o=7, while 3 and 4 are from the point r_o=8. Again, trajectories emitted at the same point with the same energy but different α values form an envelope.

Figures 17 and 18 show some skew trajectories in the coordinates r and z. Figure 17 is for 10-unit spacing, and Figure 18 is for 19-unit spacing. As r equals $\sqrt{x^2+y^2}$, it has always positive sign though x and/or y may change sign. The curves in these graphs

show radial distances from the axis. Figure 19 is a projection of the three trajectories of Figure 18 on the xy-plane.

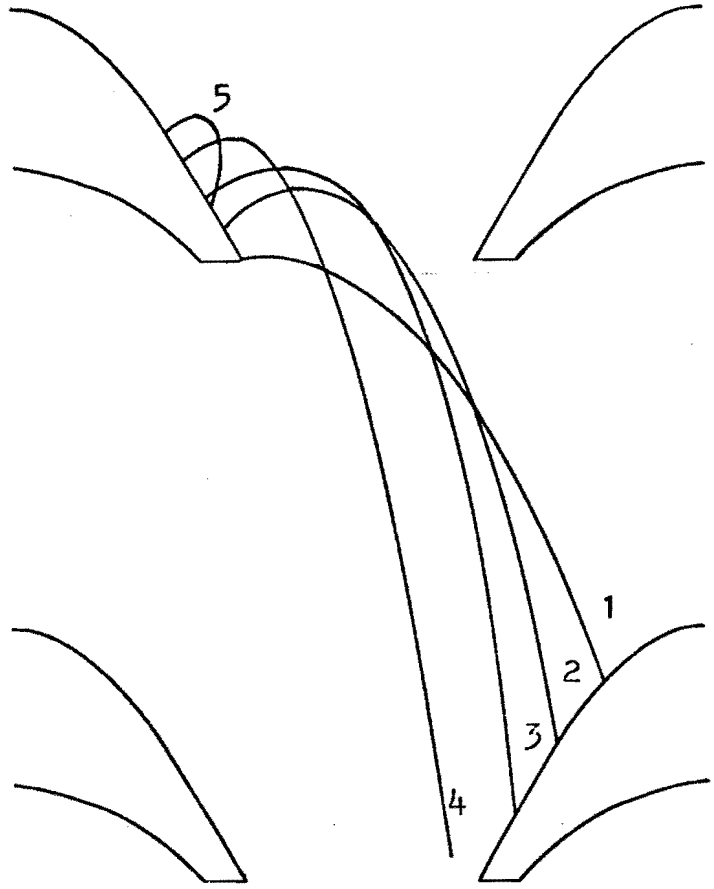

	r_o	E	α	β
1	6	3%	120°	180°
2	7	3%	120°	180°
3	8	3%	120°	180°
4	9	3%	120°	180°
5	10	3%	120°	180°

Figure 11. Meridional trajectory plots for the 19-unit spacing model for different initial positions.

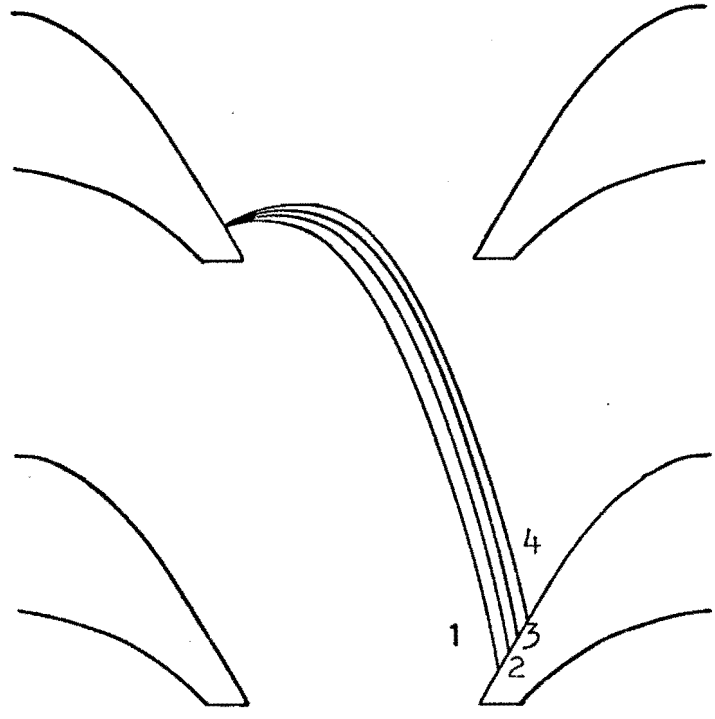

	r_o	E	α	β
1	7	1%	120°	180°
2	7	2%	120°	180°
3	7	3%	120°	180°
4	7	4%	120°	180°

Figure 12. Meridional trajectory plots for the 10-unit spacing model for different initial positions.

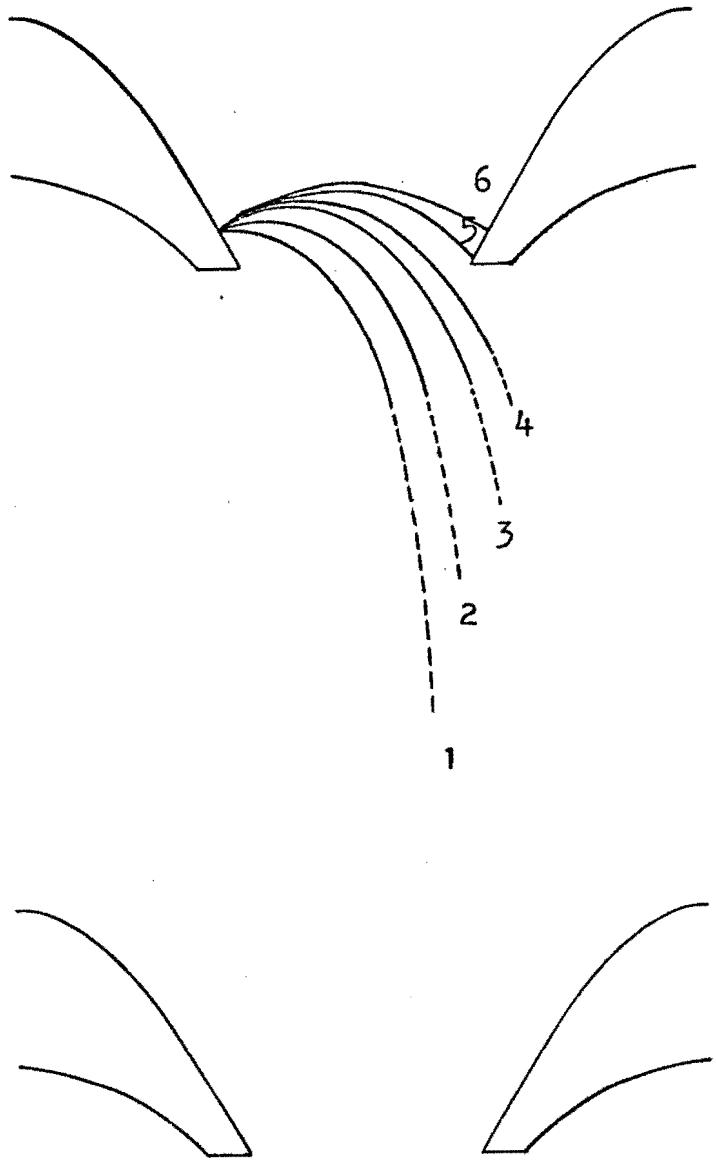

	r_o	E	α	β
1	7	0	120°	180°
2	7	1%	120°	180°
3	7	2%	120°	180°
4	7	3%	120°	180°
5	7	4%	120°	180°
6	7	5%	120°	180°

Figure 13. Meridional trajectory plots for the 33-unit spacing model for different initial energies.

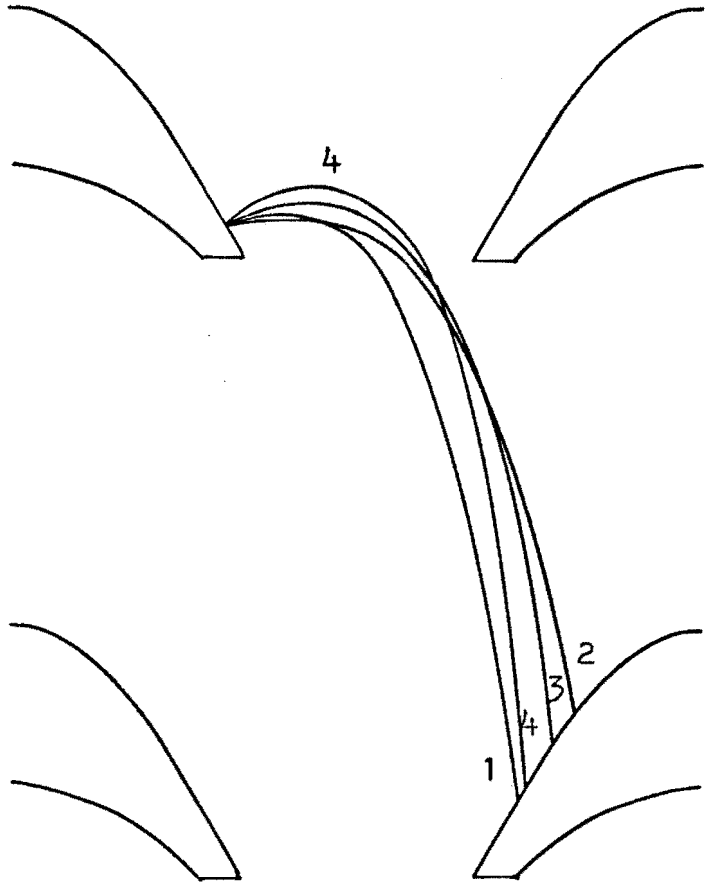

	r_o	E	α	β
1	7	1%	120°	180°
2	7	3%	110°	180°
3	7	3%	120°	180°
4	7	3%	130°	180°

Figure 14. Meridional trajectory plots for the 19-unit spacing model for different initial energies and directions.

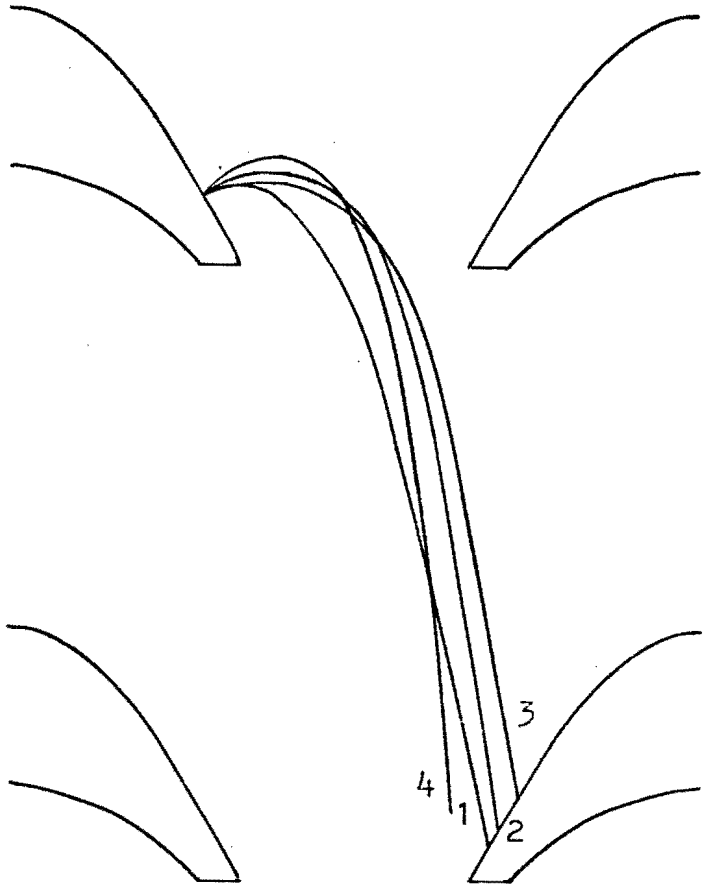

	r_o	E	α	β
1	8	1%	120°	180°
2	8	3%	120°	180°
3	8	3%	110°	180°
4	8	3%	130°	180°

Figure 15. Meridional trajectory plots for the 19-unit spacing model for different initial energies and directions.

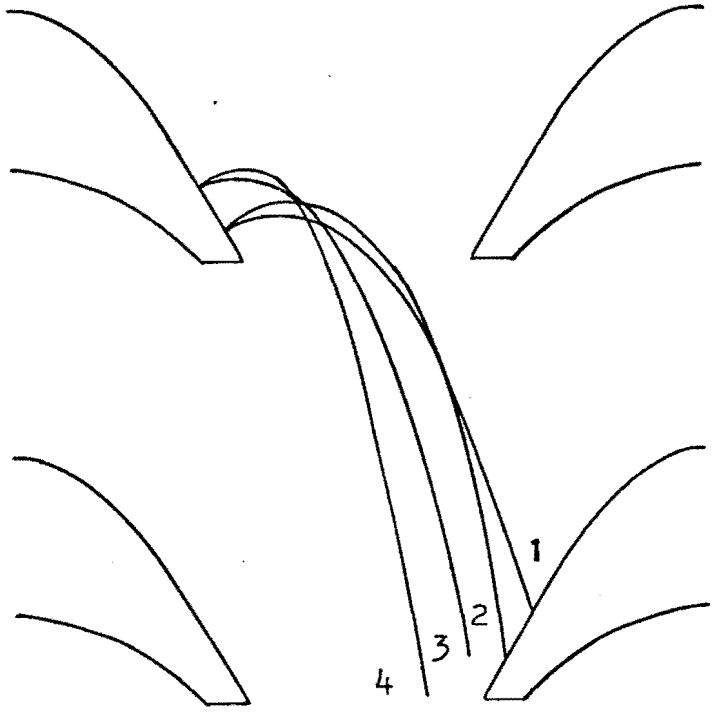

	r_o	E	α	β
1	7	3%	110°	180°
2	7	3%	130°	180°
3	8	3%	110°	180°
4	8	3%	130°	180°

Figure 16. Meridional trajectory plots for the 10-unit spacing model for different initial positions and directions.

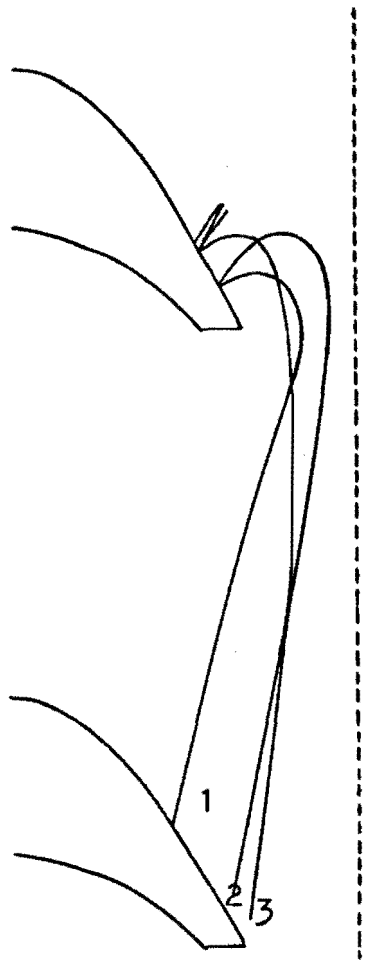

	r_o	E	α	β
1	7	3%	120°	210°
2	7	3%	150°	200°
3	8	3%	120°	210°
4	8	3%	150°	190°
5	8	3%	150°	200°

Figure 17. Skew trajectory plots for the 10-unit spacing model for different initial positions and directions.

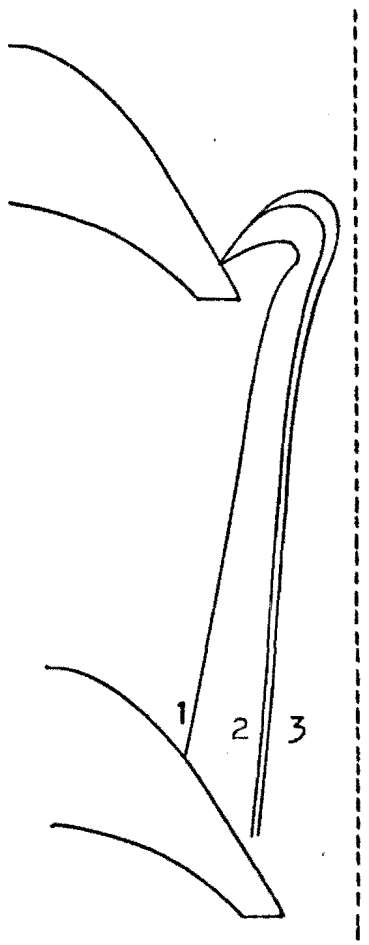

	r_o	E	α	β
1	7	3%	120°	150°
2	7	3%	150°	200°
3	7	3%	150°	190°

Figure 18. Skew trajectory plots for the 19-unit spacing model for different initial directions.

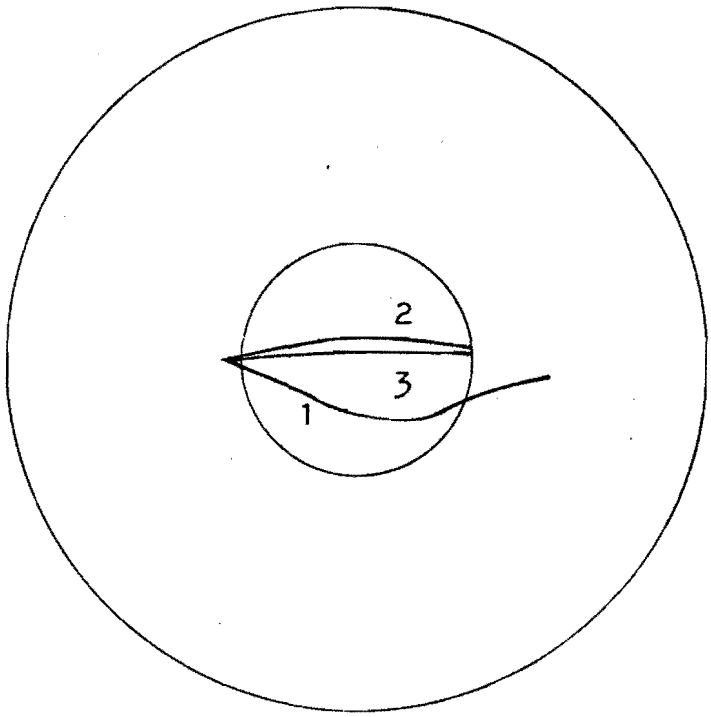

	r_o	E	α	β
1	7	3%	120°	150°
2	7	3%	150°	200°
3	7	3%	150°	190°

Figure 19. Skew trajectories projected onto the XY-plane.

CONCLUSION

The electron gain of a conical hole type multiplier structure was studied by computing the potential distribution and some electron trajectories. The only parameter, the influence of which was studied, was the spacing between two successive stages. It was found that the smallest spacing studied of approximately 77% of the electrode thickness has two important advantages compared to larger spacings: firstly, the active region where the field strength on the surface pulls the electrons into the vacuum instead of pushing them back to the electrode is wider than in the case of larger spacing; secondly, the pulling field is strong enough to collect electrons with initial energies of more than 5% of the accelerating voltage, while for larger spacings a smaller fraction of the energy distribution is collected onto the next stage. It is concluded that the conical hole type multiplier structure is feasible with sufficient gain if the spacing is chosen sufficiently small.

BIBLIOGRAPHY

Abramowitz, Milton and Irene A. Stegun. Handbook of Mathematics Functions. (National Bureau of Standards, Applied Mathematics Series 55.) Washington D.C.: Government Printing Office, 1964. Formula No. 25.2.2, page 878.

Becker, Richard and Fritz Sauter. Electromagnetic Field and Interactions. Volume I. New York: Blaisdell Publishing Co., 1964. Formula No. 13.4a, page 39.

Lenz, Friedrich A. Lectures on Electron Optics. Beaverton, Oregon: Tektronix, Inc., 1968.

Lenz, Friedrich A. A Program in Fortran IV CCS (Tymshare) Language for Electron Trajectories in Axisymmetric Electrostatic Fields. Beaverton, Oregon: Tektronix, Inc., 1970.

Southwell, Richard Vynne. Relaxation Methods in Theoretical Physics. (Oxford Engineering Science Series.) Oxford, England: Clarendon Press, 1956.

APPENDIX A

COMPUTER PROGRAM (IBM 1130) FOR POTENTIAL DISTRIBUTION

```
// JOB
// DUP
*STOREDATA  WS  UA  SHENF    2
// JOB
// DUP
*DELETE              SHEN
// FOR
*ONE WORD INTEGERS
*IOCS(PLOTTER)
*IOCS(CARD)
*IOCS(DISK)
*IOCS(TYPEWRITER)
*IOCS(1132 PRINTER)
      DIMENSION M2(17,36)
      COMMON M(17,36),MM(250,2),ICON(40),CONTB(40,2)
      DEFINE FILE 1(37,17,U,IBM)
      READ(2,507)IW,IH,LSTR
  507 FORMAT(3I2)
      IH1=IH-1
      IH2=IH-2
      WRITE(1,506)
  506 FORMAT('SW. 4 DOWN CONTINUATION RUN,UP FOR INITIAL RUN'//)
      PAUSE
      CALL DATSW(4,INT)
      GO TO (57,40),INT
   40 READ(1'1)ITR
      DO 41 I=1,IH1
      K=I+1
```

```
   41 READ(1'K)(M(J,I),J=1,IW)
      WRITE(3,502)
      GO TO 157
   57 ITR=0
157   N20 =19
      JGO=1
      WRITE(3,502)
  502 FORMAT('1')
      CALL CHEN1
   58 DO 70 I=1,IW
      DO 70 J=1,IH
   70 M2(I,J)=M(I,J)
      DO 15 J=2,IH2
      CALL DATSW(5,KGO)
      GO TO (428,430),KGO
  428 CALL CHEN2(IW,IH)
  430 IF(J-3)429,300,429
  300 DO 115 I=1,IW
  115 M(I,IH1)=(M(I,2)-M(I,1))+M(I,IH2)
  429 IF(J-4)329,330,329
  330 DO 331 I=1,IW
  331 M(I,IH)=M(I,3)-M(I,2)+M(I,IH1)
  329 DO 15 I=1,IW
      NUMEL=I*100 +J
      K=0
   59 K=K+1
      IF(MM(K,1)-9999)60,62,62
   60 IF(MM(K,1)-NUMEL)59,61,59
   61 LAW=MM(K,2)
      GO TO 63
   62 LAW=1
   63 IF( 5-LAW) 8,64,64
   64 GO TO (1,2,3,4,5),LAW
    1 IB=M(I,J+1)
  101 IA=M(I-1,J)
```

```
          C=M(I+1,J)
          ID=M(I,J-1)
          M(I,J)=((IA+IB+ C+ID)/4)+(( C-IA)/(8*(I-1)))+.5
        2 GO TO 15
        3 IB=0
          GO TO 101
        4 IB=M(I,J+1)
          C=M(I+1,J)
          ID=M(I,J-1)
          M(I,J)=((4* C+IB+ID)/6.)+.5
          GO TO 15
        5 A=M(I-1,J)
          IB=M(I,J+1)
          ID=M(I,J-1)
          M(I,J)=((2* A+IB+ID)/4.)+.5
          GO TO 15
        6 M(I,J)=   AC*M(I,J-1)+.5
          GO TO 15
        7 M(I,J)=   AC*M(I-1,J)+.5
          GO TO 15
        8 ISUB=LAW-5
          NWLAW=ICON(ISUB)
          AC=CONTB(ISUB,1)
          BC=CONTB(ISUB,2)
          GO TO (11,10,9,12,6,7),NWLAW
C*********************180
        9 IA=M(I-1,J)
          IB=M(I-2,J)
          GO TO 13
C*********************  90
       10 IA=M(I,J+1)
          IB=M(I,J+2)
          GO TO 13
C*********************   0
       11 IA=M(I+1,J)
```

```
      IB=M(I+2,J)
      GO TO 13
C***************** 270
   12 IA=M(I,J-1)
      IB=M(I,J-2)
   13 M(I,J)=(IA*AC-IB*BC )+.5
   15 CONTINUE
      ITR=ITR+1
      DO 30 I=1,IW
   30 M(I,1)=M(I,IH2)-M(I,IH1)+M(I,2)
      N20=N20+1
      IF(N20-20)36,35,36
   35 WRITE(3,505)ITR
      CALL CHEN2(IW,IH)
      N20=0
   36 DO 20 I=1,IW
      DO 20 J=2,IH2
      IF (M(I,J)-M2(I,J))25,20,25
   20 CONTINUE
      WRITE(3,500)
  500 FORMAT(' THIS IS THE FINISHED MATRIX')
      JGO=2
      GO TO 26
   25 CALL DATSW(1,NPRT)
      GO TO (26,28),NPRT
   26 WRITE(3,505)ITR
  505 FORMAT(50X,'ITERATION ',I5,//)
      CALL CHEN2(IW,IH)
   28 CALL DATSW(6,IEND)
      GO TO (24,29),IEND
   24 WRITE(1,1)ITR
      DO 22 I=1,35
      K=I+1
   22 WRITE(1,K)(M(J,I),J=1,IW)
      WRITE(3,508)ITR
```

```
 508 FORMAT(20X,I5' IS THE ITR. STORED FOR CONTINUATION RUN'//)
     CALL CHEN2(IW,IH)
     GO TO 38
  29 GO TO (58,27),JGO
  27 NCT=0
     WRITE(1,501)
 501 FORMAT('SW 10 UP FOR PLOT.')
     PAUSE
     CALL DATSW(10,KPLOT)
     GO TO(170,71),KPLOT
 170 CALL POPS(IW,IH)
  71 CALL XTRAP(IW,LSTR)
     CALL CHEN2(IW,IH)
     DO 200 I=1,120
 200 CALL PASK8(16448,IE)
     DO 201 I=1,120
 201 CALL PASK8(1856,IE)
     DO 250 J=1,LSTR
     IY=LSTR-J+1
     DO 250 I=1,IW
     IX=IW-I+1
     CALL FILL (ICON,1,6,-4032)
     NUM=M(IX,IY)
     IF(NUM)202,204,203
 202 NUM=-1*NUM
     ICON(1)=24640
 203 CALL MSIA(ICON,2,6,NUM,0)
 204 DO 205 IP=1,6
 205 CALL PASK8(ICON(IP),IE)
     NCT=NCT+1
     IF(J-LSTR)207,206,206
 206 IF(I-IW)207,208,208
 207 CALL PASK8 (27456,IE)
 208 IF(NCT-9)250,209,209
```

```
  209 NCT=0
      CALL PASK8(3392,IE)
      CALL PASK8(9536,IE)
  250 CONTINUE
      DO 251 I=1,240
  251 CALL PASK8(16448,IE)
      WRITE(1,509)
  509 FORMAT('SW 2 UP CALL EXIT'/'      DOWN NEW SHEN JOB'/)
      PAUSE
      CALL DATSW(2,NGO)
      GO TO (38,57),NGO
   38 CALL EXIT
      END
// DUP
 *STORE      WS  UA  SHEN
```

```
// JOB
// DUP
 *DELETE              CHEN1
// FOR
 *ONE WORD INTEGERS
      SUBROUTINE CHEN1                                                  00
      COMMON M(17,36),MM(250,2),ICON(40),CONTB(40,2)
      I=1                                                               20
C  READ IN TABLE OF POINT-LAW RELATIONS  9999 POINT DENOTE END OF TABLE  35
   10 READ (2,101) MM(I,1),MM(I,2)                                      45
  101 FORMAT (I4,I2)                                                    50
      IF(MM(I,1)-9999) 15,20,15                                         55
   15 I=I+1                                                             60
      GO TO 10                                                          65
C  TABLE FILLED                                                         70
C---READ IN LAW TABLE  DUMMY LAST CARD HAS 9 IN COL 1                  00
   20 CONTINUE
      L=1                                                               05
```

```
    60 READ (2,102) ICON(L),CONTB(L,1),CONTB(L,2)                          10
  102 FORMAT (I1,2F6.4)                                                    15
                IF (ICON(L)-9) 62,63,62                                    20
   62 L=L+1                                                                25
      GO TO 60                                                             30
   63 CONTINUE                                                             35
C *********THIS SECTION READS IN 35 CARDS****EACH CARD INITIALIZES A
C                  HORIZONTAL ROW TO THE VALUE IN COLUNNS 1-5 IN THE CARD
      CALL DATSW(4,IGO)
      GO TO (70,80),IGO
 70   DO 700 KA=1,35
      READ(2,680) MLT
  680 FORMAT(I6)
      DO 700 KB=1,17
  700 M(KB,KA)=MLT
C     ************ END OF INITIALIZATION SECTION
  701 READ(2,103)IX,IY,INV
  103 FORMAT (2I2,I6)
      IF(IX-99)702,80,702
  702 M(IX,IY)=INV
      GO TO 701
 80   RETURN                                                               45
      END                                                                  50
// DUP
 *STORE       WS  UA  CHEN1
// JOB
// DUP
*DELETE            CHEN2
// FOR
*ONE WORD INTEGERS
      SUBROUTINE CHEN2 (IX,IY)                                             00
      COMMON M(17,36),MM(250,2),ICON(40),CONT(40,2)
      JACK=IY+1
      DO 50 J=1,IY
      N=JACK-J
```

```
     50 WRITE (3,101)          (M(K,N),K=1,IX)
    101 FORMAT(1X,17(I5,2X))
        WRITE (3,102)                                                    70
    102 FORMAT(1H1,1X)                                                   75
        RETURN                                                           80
        END                                                              85
// DUP
 *STORE       WS  UA  CHEN2
```

APPENDIX B

POTENTIAL DISTRIBUTION (10-UNIT SPACING)

-3915	-3908	-3886	-3847	-3791	-3717	-3623	-3508	-3372	-3215	-3040	-2850	-2651	-2454	-2274	-2141	-2091
-3383	-3375	-3351	-3308	-3247	-3167	-3065	-2941	-2793	-2621	-2424	-2203	-1960	-1702	-1443	-1224	-1135
-2884	-2876	-2850	-2805	-2741	-2656	-2549	-2418	-2260	-2072	-1853	-1599	-1305	-970	-590	-187	0
-2425	-2417	-2391	-2345	-2279	-2192	-2082	-1946	-1781	-1582	-1345	-1062	-722	-315	0	0	0
-2006	-1998	-1972	-1927	-1862	-1776	-1667	-1530	-1363	-1160	-914	-614	-242	0	0	0	0
-1627	-1619	-1594	-1552	-1490	-1408	-1303	-1171	-1008	-810	-569	-273	0	0	0	0	0
-1284	-1277	-1255	-1217	-1161	-1086	-989	-867	-716	-532	-310	-43	0	0	0	0	0
-976	-970	-952	-920	-873	-809	-724	-616	-482	-319	-124	0	0	0	0	0	0
-696	-692	-679	-656	-621	-571	-503	-414	-301	-163	0	0	0	0	0	0	0
-437	-436	-430	-419	-399	-368	-321	-254	-165	-53	0	0	0	0	0	0	0
-190	-192	-195	-199	-200	-193	-173	-133	-70	0	0	0	0	43	171	245	269
57	52	37	14	-13	-39	-54	-47	-13	0	0	0	155	352	485	562	586
324	314	285	238	175	103	40	6	0	0	0	228	510	713	849	927	952
628	614	570	495	387	251	112	11	0	0	249	639	925	1129	1265	1342	1367
989	971	915	815	657	428	165	0	0	189	734	1123	1403	1601	1733	1807	1831
1420	1401	1343	1234	1045	689	0	0	0	819	1329	1685	1943	2127	2250	2320	2343
1924	1909	1863	1783	1667	1528	1488	1256	1321	1686	2034	2318	2539	2702	2814	2878	2899
2487	2477	2443	2401	2342	2284	2256	2225	2316	2532	2773	2993	3177	3319	3419	3478	3497
3087	3082	3068	3049	3029	3019	3030	3068	3168	3328	3510	3687	3843	3969	4061	4116	4134
3705	3704	3703	3704	3711	3731	3772	3839	3943	4081	4235	4388	4528	4646	4734	4788	4806
4324	4326	4334	4350	4376	4417	4477	4560	4669	4800	4944	5089	5226	5345	5437	5494	5513
4932	4937	4951	4977	5016	5072	5146	5241	5357	5491	5637	5787	5932	6063	6168	6236	6259
5522	5528	5547	5580	5629	5695	5780	5885	6010	6153	6311	6476	6642	6798	6930	7020	7052
6085	6092	6114	6153	6209	6283	6377	6492	6628	6785	6960	7150	7349	7546	7726	7859	7909
6617	6625	6649	6692	6753	6833	6935	7059	7207	7379	7576	7797	8040	8298	8557	8776	8865
7116	7124	7150	7195	7259	7344	7451	7582	7740	7928	8147	8401	8695	9030	9410	9813	10000

APPENDIX C

POTENTIAL DISTRIBUTION (19-UNIT SPACING)

-2269	-2265	-2252	-2230	-2199	-2159	-2109	-2049	-1979	-1899	-1808	-1708	-1602	-1494	-1393	-1317	-1288
-1955	-1951	-1937	-1913	-1880	-1837	-1782	-1716	-1637	-1544	-1437	-1315	-1179	-1031	-880	-750	-697
-1660	-1656	-1641	-1616	-1581	-1535	-1477	-1406	-1319	-1216	-1093	-949	-780	-584	-358	-114	0
-1388	-1384	-1369	-1344	-1308	-1261	-1201	-1126	-1034	-923	-789	-626	-428	-188	0	0	0
-1140	-1136	-1122	-1098	-1062	-1015	-955	-879	-786	-671	-531	-358	-141	0	0	0	0
-916	-912	-899	-876	-843	-798	-740	-667	-576	-464	-327	-157	0	0	0	0	0
-714	-711	-699	-679	-650	-609	-556	-489	-405	-301	-176	-24	0	0	0	0	0
-532	-530	-520	-504	-480	-446	-401	-342	-268	-177	-68	0	0	0	0	0	0
-366	-365	-359	-348	-331	-306	-271	-224	-163	-88	0	0	0	0	0	0	0
-212	-212	-211	-208	-201	-187	-165	-132	-86	-27	0	0	0	0	0	0	0
-64	-66	-71	-78	-83	-85	-80	-63	-33	0	0	0	0	27	106	152	166
85	81	69	50	27	4	-12	-16	-5	0	0	0	96	217	299	346	361
251	244	223	188	142	89	41	11	0	0	0	141	314	438	521	569	584
445	435	404	351	275	180	82	8	0	0	154	393	568	692	774	821	836
678	666	627	557	449	293	113	0	0	117	453	691	860	979	1058	1102	1116
961	948	907	831	702	463	0	0	0	511	823	1038	1191	1299	1371	1411	1424
1295	1284	1251	1193	1109	1008	969	808	839	1058	1264	1430	1556	1648	1710	1745	1757
1673	1665	1642	1604	1555	1504	1470	1434	1474	1593	1726	1847	1945	2020	2072	2102	2112
2081	2076	2062	2042	2014	1991	1979	1982	2022	2099	2189	2276	2351	2410	2452	2477	2485
2508	2505	2497	2487	2476	2469	2472	2488	2525	2581	2646	2710	2767	2813	2846	2866	2872
2944	2943	2940	2937	2935	2938	2949	2970	3003	3047	3096	3145	3189	3225	3251	3267	3272
3383	3383	3383	3385	3389	3389	3413	3435	3465	3501	3540	3579	3614	3643	3665	3678	3682
3820	3821	3824	3829	3837	3849	3866	3888	3915	3947	3980	4012	4042	4066	4085	4096	4099
4254	4255	4259	4266	4277	4291	4309	4332	4358	4387	4417	4446	4472	4494	4510	4520	4523
4681	4683	4688	4696	4709	4725	4745	4768	4795	4823	4851	4879	4904	4925	4940	4950	4953
5101	5103	5109	5119	5133	5151	5173	5198	5226	5255	5284	5312	5337	5359	5375	5385	5388
5513	5515	5522	5533	5549	5569	5593	5621	5651	5682	5714	5744	5772	5796	5814	5825	5829
5914	5917	5925	5937	5955	5978	6005	6036	6070	6105	6141	6176	6208	6236	6258	6271	6276
6305	6308	6317	6331	6351	6377	6408	6443	6482	6523	6565	6607	6646	6681	6708	6725	6731
6684	6687	6697	6713	6736	6765	6800	6840	6885	6934	6985	7036	7085	7130	7165	7188	7196
7049	7053	7064	7082	7107	7139	7179	7225	7278	7336	7398	7462	7525	7584	7632	7664	7675
7399	7403	7415	7435	7463	7499	7544	7597	7658	7726	7801	7882	7964	8043	8112	8160	8177
7731	7735	7748	7770	7801	7841	7891	7951	8021	8101	8192	8292	8398	8506	8607	8683	8712
8045	8049	8063	8087	8120	8163	8218	8284	8363	8456	8563	8685	8821	8969	9120	9250	9303
8340	8344	8359	8384	8419	8465	8523	8594	8681	8784	8907	9051	9220	9416	9642	9886	10000

APPENDIX D. POTENTIAL DISTRIBUTION (33-UNIT SPACING)

-1083		-1070		-1030		-960		-855		-707	-504	-234	0
-763		-750		-709		-635		-519		-347	-89	0	0
-496		-485		-449		-383		-276		-116	0	0	0
-275		-268		-246		-201		-121		0	0	0	0
-176	-176	-173	-169	-162	-150	-131	-104						
-80	-80	-82	-84	-84	-81	-73	-56	-30		0	0	60	95
19	17	11	-1	-10	-20	-25	-21	6		0			
127	123	112	92	67	39	14	2	0		0	177	305	342
251	245	228	197	154	100	44	4	0					
398	391	369	328	264	172	66	0	0	69	244	505	629	664
576	568	544	499	422	278	0	0	0	306	488	618		
786	779	759	724	674	614	592	492	509	640	767	938	1029	1056
1022	1017	1003	980	950	919	898	873	894	964				
1277	1274	1266	1252	1235	1220	1210	1208	1226		1333	1429	1486	1504
1546	1544	1539	1531	1523	1517	1516	1522						
1822		1818		1812		1814		1838		1892	1944	1979	1990
2380		2380		2382		2391		2411		2442	2471	2491	2498
2939		2940		2944		2953		2968		2987	3004	3016	3020
3493		3494		3498		3506		3517		3529	3540	3547	3550
4042		4043		4047		4053		4061		4070	4077	4082	4084
4585		4586		4590		4595		4602		4610	4616	5620	4621
5123		5124		5128		5134		5141		5149	5155	5159	5160
5655		5657		5662		5669		5678		5687	5695	5700	5702
6180		6182		6189		6199		6212		6225	6236	6244	6246
6694		6697		6707		6722		6741		6761	6779	6792	6796
7194		7199		7213		7235		7264		7295	7324	7346	7354
7675		7682		7702		7734		7776		7824	7873	7911	7926
8128		8137		8164		8209		8270		8344	8425	8495	8526
8546		8557		8591		8649		8733		8842	8974	9109	9186
8917		8930		8970		9040		9145		9293	9496	9766	10000